Supporting information of the paper

# "Fluorinated imidazoles as proton carriers for water-free fuel cell membranes"

Wei-Qiao Deng, Valeria Molinero, and William A Goddard III

*Materials and Process Simulation Center, Division of Chemistry and Chemical Engineering, California Institute of Technology, Pasadena. CA, 91125*

## Computational methods and detailed calculation results

Abstract

We organized this supporting material as follows: Section 1 describes the calculation method and detailed calculation results for Pt electrode poisoning problems, and Section 2 describes the methodology employed to estimate the proton diffusion in the imidazole/nafion and trifluoroimidazole/nafion membranes.

### 1. Pt electrode poisoning problem.

In order to study the poisoning of platinum in the presence of imidazoles, we used CASTEP [1] to calculate the binding energy between imidazole derivatives and platinum surface. A periodic slab that includes two layers of platinum totalizing 8 atoms was used to describe Pt (111) surface. The unit cell c parameter was set to be 16Å at z direction for keeping 50% of the unit cell as vacuum in order to avoid any interaction between slabs. The calculations were performed by using nonlocal density functional theory (DFT) with the generalized gradient approximation (GGA-II) [2] and periodic boundary conditions. We used the norm-conserving plane wave pseudopotentials generated with the optimization scheme of Lin et al. [3] We found significant changes in relative energetics for cutoffs up to 600 eV, requiring a cutoff of 940 eV to obtain convergence. We found that a k-point sampling of 2×2×1 was sufficient for convergence. All energies were extrapolated to 0 K using the correction technique of Gillan and De Vita.[4] All calculations were performed with the CASTEP code in the CERIUS2 software package.[1]

As comparison, we also studied the CO and $H_2O$ adsorbed on the platinum surface. Figure S1 shows all detailed structures optimized by CASTEP program.

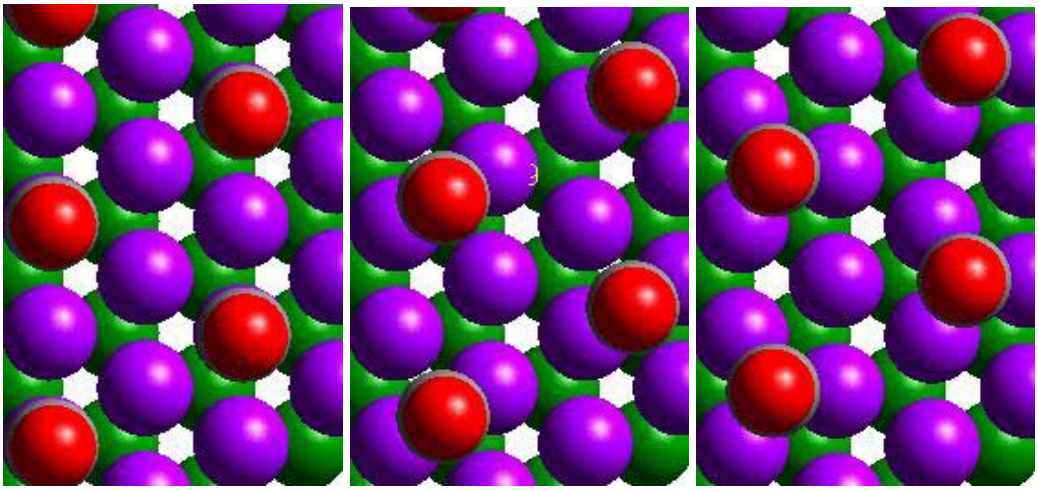

Figure S1. Structures of CO bind with Platinum 111 surface. a) top b) bridge, c) fcc hollow site. Pink atom is first layer Pt, Green is second layer Pt atom, red is oxygen atom, gray is carbon atom.

Table S1. Comparison of adsorption energies for CO on Pt computed in the current work with experimental results and other simulation results. (E in kcal/mole)

| Energy functional | Top position | Bridge position | Three fold hollow |
|---|---|---|---|
| GGAII[a] | 38.5 | 37.8 | 37.1 |
| B88/P86[b] | 53.0 | 43.1 | 38.0 |
| experiment[c] | 42.3 ± 6.7 | | |

a) this work, b) Ref 12 c) Ref. 9 of the paper.

Table S2. Comparison of bond distances of CO adsorbed on Pt surface of current work with experimental results and other simulation results. (Distances in Å)

| Energy functional | Top position | Bridge position | Three fold hollow |
|---|---|---|---|
| GGAII[a] | 1.852 | 2.021 | 2.095 |
| B88/P86[b] | 1.89 | 1.99 | |
| experiment[c] | 1.85±0.10 | 2.08±0.07 | |

a) this work, b) Ref 12 c) Ref. 13 and 14

Table S2 shows that bond distances of top position Pt-CO are in good agreement with the experimental value and the bond distances of bridge position Pt-CO is 0.020 Å shorter than experimental value.

The second calculation we used for validation was the binding of water molecule with the Pt 111 surface, that is to have considered slight or no poisoning effects. By using the same calculation method as for CO, we found that the most stable binding site has a binding energy of 11.0 kcal/mole and corresponds to water over the top position. This result compares well with the experimental value of 12.5 kcal/mole (Ref. 10 of the paper)

Imidazole molecule has an $sp^2$ lone pair orbital that is easy to bind with Pt surface vacant orbital to make large binding energy. Our DFT calculation indicates that a 1/4 coverage imidazole layer on platinum surface, whose structure is shown in Figure S3, will have 21.1 kcal/mole binding energy which is twice water's binding energy with platinum surface. The large binding energy between platinum surface and imidazole will keep activated species such as $H_2$ away from surface and thus block further reactions. To reduce the binding energy between platinum and imidazole, we consider that replacing H for an electron-acceptor such as the fluoro

groups at the ring carbons will stabilize the $sp^2$ lone pair orbital and thus increase the mismatch between $sp^2$ lone pair and platinum surface vacant orbitals, responsible for the binding. The DFT calculation results in Table S3 shows the effect of fluorination on lowering the energy of the $sp^2$ orbital from –9.9eV for imidazole (Im) to -11.3eV for 2,4,5-trifluoroimidazole (ImF3). The energy of the platinum surface vacant orbital is –5.66eV, according to the Castep calculation. As expected, the mismatch between $sp^2$ lone pair of substituted imidazole and platinum vacant surface orbital has increased with the fluorination, with a concomitant decrease in the binding energy of the molecule to the surface (see Table S3).

Table S3 Computed binding energies of water, CO, Im and ImF3 to the Pt surface.

| Energy functional | Top position Binding energy (kcal/mol) | Bond distance(Å) |
|---|---|---|
| Water | 11.0 | 2.142 |
| CO | 38.5 | 2.095 |
| Imidazole | 21.1 | 2.100 |
| 2,4,5-trifluoroimidazole | 1.3 | 2.449 |

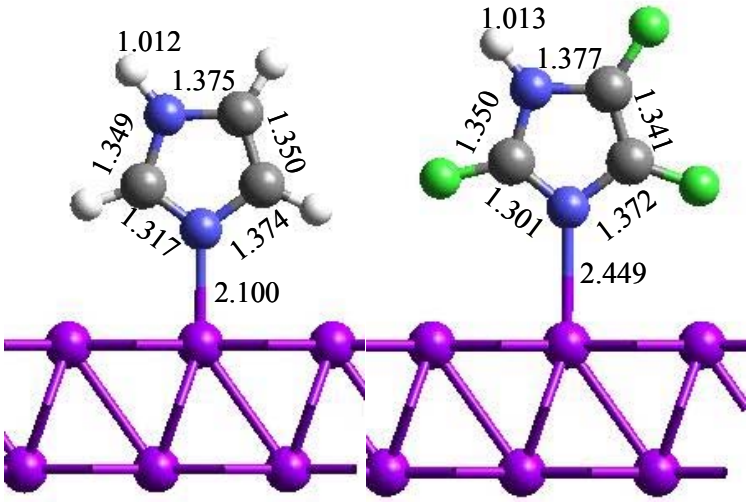


Figure S2. Binding of Im (left) and ImF3 (right) with platinum surface. The lone pair on nitrogen will strongly bind with platinum surface vacant orbitals. The color code is: Magenta for Pt, , gray for C, blue for N, green for F, and white for H.

The energies listed in Table S3 correspond to the binding energies of the monolayer to the Pt electrode. We also computed the intermolecular energy between the Im (or ImF3) in the monolayer, and found that is less than 1 kcal/mole.

We have considered other geometries for the binding of the Im and ImF3 to the Pt surface, and we found that the binding with the molecule plane perpendicular to the surface, with the bare N over a top position of the Pt 111 provides the highest binding energy. The binding energies of ImF3 perpendicular to the surface with the N over the three-fold FCC site is 0.92 kcal/mole, over the bridge site is 0.57 kcal/mole. We have also considered the binding of the ImF3 molecule parallel to the Pt surface, and found that the binding energy is even lower than the observed for the perpendicular geometry, confirming the absence of any poisoning effect of the ImF3 on Pt.

**2. Proton transport**

## 2.1 Molecular dynamics simulations of Im and ImF3 impregnated Nafion membranes, and water-$H3O^+$ system

In this section we describe the methodologies used to investigate the proton diffusion in the imidazole and trifluoroimidazole impregnated Nafion membranes, and for hydronium in water

**Molecular Dynamics methods and force fields.**

The Nafion/imidazole systems were modeled with fully atomistic detail using classical Molecular Dynamics in the canonical (NVT) and isobaric-isothermal ensemble (NPT). The calculations were performed using LAMMPS (Large-scale Atomic/Molecular Massively Parallel Simulator) code from Plimpton at Sandia [4,5], which was modified to handle our force fields.[9,11] The equations of motion were integrated using the Verlet algorithm[6] ith a time steps of 1.0 fs, and the Particle-Particle Particle-Mesh (PPPM) method[7] was used for long range electrostatic interactions in the periodic cells.

The inter- and intramolecular interactions were described through the DREIDING force field [8] in the version that improves the description of the fluorocarbon moieties [9]. Water is modeled using the F3C force field.[10] The force field details, charges, parameters, and application in the study of the structure and dynamics of hydrated Nafion membranes has been extensively described in a recent publication.[11] The imidazole, imidazolium, trifluoroimidazole and trifluoroimidazolium force field parameters correspond to the original DREIDING force field. The partial charges on the atomic sites of imidazole and trifluoroimidazole correspond to the Mulliken charges computed from Quantum Mechanics optimization of the molecules in vacuum using B3LYP/6-311G** and are listed in Table S4.

We have prepared periodic simulation cells containing each four ionized Nafion chains, 40 protonated imidazolium (ImH+) (or trifluoroimidazolium, (ImF3H+)) and 80 neutral Im or ImF3. Each chain had the dispersed sequence [11] $(N_7P)_{10}$, were $N$=($CF_2$-$CF_2$) are the nonpolar TFE segments, and $P$=($CF_2$-CF(O-$CF_2$-CF($CF_3$))-$CF_2$-$CF_2$-$SO_3H$) are the polar perfluorosulfonic vinyl ether (PSVE) segments,. The total number of atoms in each system was 3848. The proportion of 3 Im molecules per sulfonate of the Nafion chain corresponds to ~15%wt.

Table S4. The atomic charges for imidazoles and protonated imidazoles.

| | $ImH^+$ | Im | $ImF3H^+$ | ImF3 |
|---|---|---|---|---|
| $N_1$ | -0.1953 | -0.5479 | -0.2838 | -0.6311 |
| $C_2$ | 0.1446 | 0.2063 | 0.4642 | 0.6701 |
| $N_3$ | -0.1953 | -0.4228 | -0.2838 | -0.4809 |
| $C_4$ | -0.0978 | -0.0301 | 0.2500 | 0.4067 |
| $C_5$ | -0.0978 | 0.01816 | 0.2500 | 0.4217 |
| $H_1$ | 0.3666 | 0.3344 | 0.4097 | 0.3638 |
| $H_2/F_2$ | 0.2452 | 0.1546 | -0.0827 | -0.2402 |
| $H_3$ | 0.3666 | ---- | 0.4097 | --- |
| $H_4/F_4$ | 0.2316 | 0.1354 | -0.0667 | -0.2583 |
| $H_5/F_5$ | 0.2316 | 0.1520 | -0.0667 | -0.2517 |

The label of the atoms for the charge assignment is indicated in the following scheme:

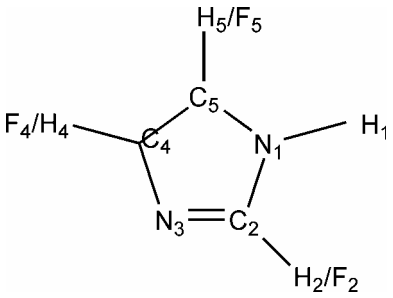

The ImF3/Nafion membranes were created and equilibrated as follows: we started from an equilibrated structure of hydrated Nafion, completely ionized, with 15 water molecules per sulfonate (~20%wt) at 353 K prepared as indicated in Reference [11], then the 560 water and 40 hydronium molecules were removed from the structure, and the polymer was loaded with i) 80 imidazole and 40 imidazolium, or ii) 80 trifluoroimidazole and 40 trifluoroimidazolium. We used the Monte Carlo procedure of Cerius2 Sorption Module [1] to load the molecules into the cell. The method was operated at fix load, and $10^5$ Monte-Carlo steps were used to optimize the structures. The system was then equilibrated for 500 ps, performing a NPT dynamics at 450 K. The equilibration of the system was verified monitoring time dependence of the energy and density. Then, an 1 ns equilibrium NPT MD simulation at 450 K was run for each of the two systems. The equilibrium data of this work was collected from these 1 ns trajectories for each of the proton carriers.

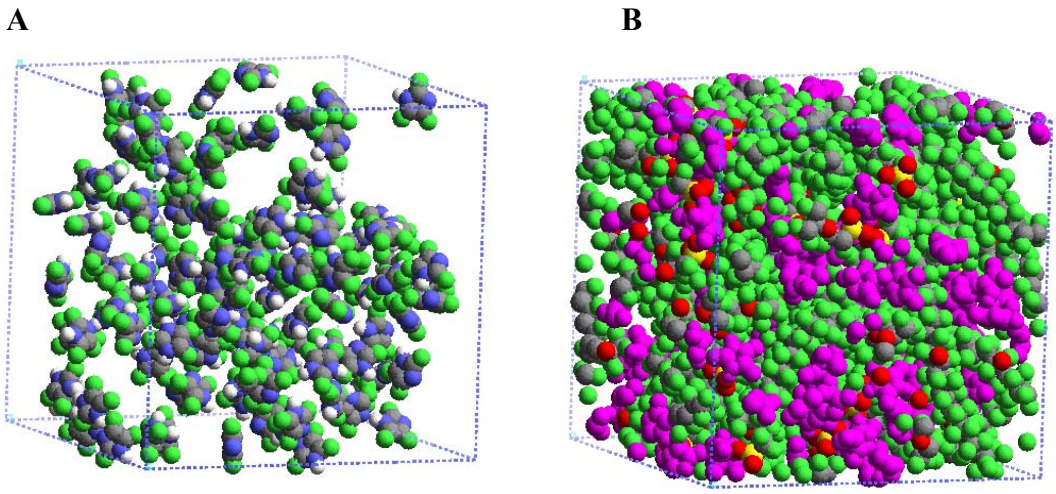


Figure S3. Typical configuration of ImF3/nafion that illustrates the structure of the membrane. A) Protonated (ImF3H+) and neutral (ImF3) carrier molecules, polymer

hidden. B) Same configuration, showing the carriers (all in magenta) and the nafion chains.

The simulation of **$H_3O^+$ in water** was done using the force field described in reference [11] for the hydrated ionized Nafion membrane. The simulation cell consisted of 200 water molecules, 1 $H_3O^+$ and 1 $CF_3$-$CF_2$-$SO_3^-$. We simulated the system using NPT MD dynamics at 300 K and 1 bar using the code and methods describe above for the membranes. The simulation time was of 2 ns, and we collected statistical for the study the diffusion during the last 1.5 ns of the trajectory.

**2.2 Estimation of the proton diffusion coefficient.**

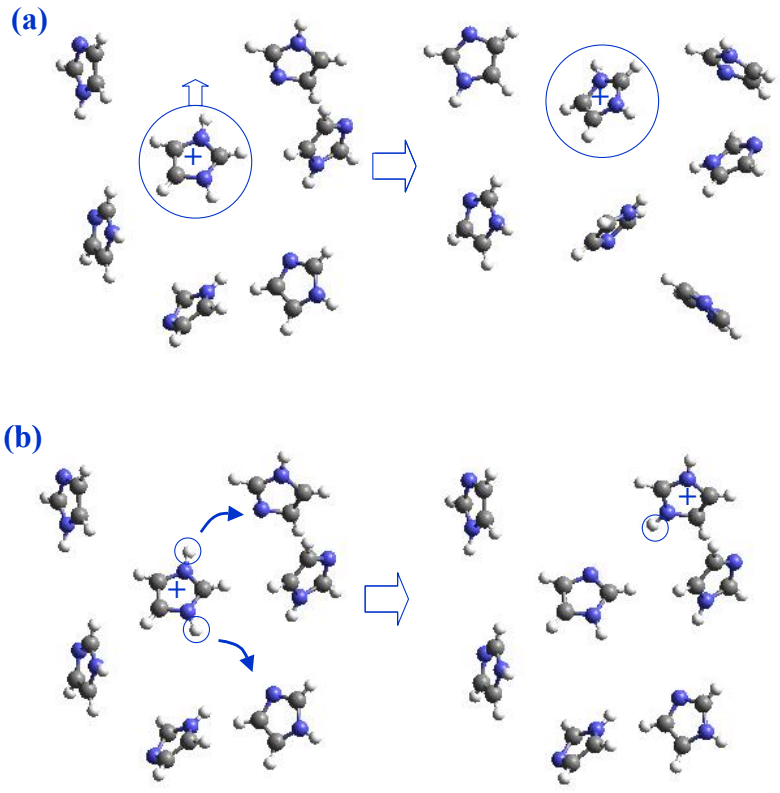

Figure S4. The scheme of proton diffusion mechanism. a) vehicular mechanism, protonated imidazole diffuse in the solvent. b) hopping mechanism, proton hops from one carrier to another

The proton diffusion mechanism includes the combination of two mechanisms, i.e., the vehicular mechanism and hopping mechanism. We use molecular dynamics (MD) to study protonated species, e.g., protonated imidazole and hydronium vehicular diffusion coefficients in Nafion.

**2.2.1. Vehicular diffusion of protonated species.**

The vehicular diffusion of the protonated molecules was calculated from the slope of the mean square displacement (MSD) with time:

$$D^{MSD} = \lim_{t\to\infty} \frac{\left\langle \left|\vec{r}(t) - \vec{r}(0)\right|^2 \right\rangle}{6t} \tag{1}$$

where r is the position vector and t is the time, and the brackets indicate an average over all the protonated carriers in the system and over the equilibrium trajectory. The resultant coefficient for the vehicular diffusion for hydronium, imidazolium, and trifluoroimidazolium are indicated in Table 1 of the paper.

**2.2.2 Hopping contribution to proton diffusion.**

The proton transfer rate k(r) between a proton donor and a proton acceptor carrier was computed using transition state theory (TST) with the WKB [12] correction for proton tunneling.

$$k(r) = \kappa(T,r)\frac{k_B T}{2\pi\hbar}\exp\left(-\frac{E_b(r) - \hbar\omega_1(r)/2}{k_B T}\right)$$

where r is the distance between the donor and acceptor N atoms of the two molecules, $E_b(r)$ is the energy barrier to transfer the proton between these N atoms, and $\omega_1(r)$ is the frequency of the zero point energy correction.

We use B3LYP/6-311G**++ to scan the potential energy curves for the proton hopping reaction between a protonated and noprotonated (substituted) imidazole. Then, the determined structures at the minima and the saddle points were reoptimized by using the Jaguar's Poisson-Boltzmann Self-Consistent Reaction Field model (PB-SCRF). The hopping barrier corresponds to the energy difference between minima and saddle points calculated in solvent media. The experimental dielectric constant for imidazole[15] $\varepsilon$=23.0, has been used in modeling the solvent. The probe radius is 2.6 Å for imidazole. To validate the theoretical model with a well known system, we also calculated the hopping barrier for the proton between two water molecules using PB-SCRF, with the dielectric constant of water $\varepsilon$=80.37, and a probe radius of 1.4 Å. The coordinates of energy curves are the N-N distance $R_1$ and the proton-oxygen distance $R_2$ (Figure S5). For each curve, $R_1$ is kept constant while $R_2$ is increased in increments of 0.01 Å. The calculated potential energy curves for several values of $R_1$ are displayed in Figure S5. The activation energy defined as the energy difference between the maximum and minimum points of the curve, decreases significantly as R(N-N) decreases. At fixed $R_1$, the left minimum corresponds to the equilibrium of a left imidazole molecule with a right protonated imidazole, whereas the symmetric minimum located at the right corresponds to a left protonated imidazole in equilibrium with a right imidazole molecule. A transition state for proton transfer corresponds to the maximum point in Figure S5, i.e., a proton is located equidistant between the two imidazole molecules. From Figure S5, we observe that, with the increase of the R(N-N) distance, the activation barrier for proton transfer increases sharply, and at a certain small R(N-N) value, the transfer is barrier free. Our results indicate that the proton hopping barrier is barely affected by the fluorination.

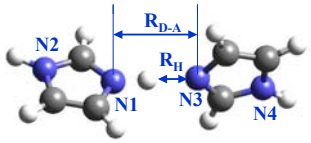


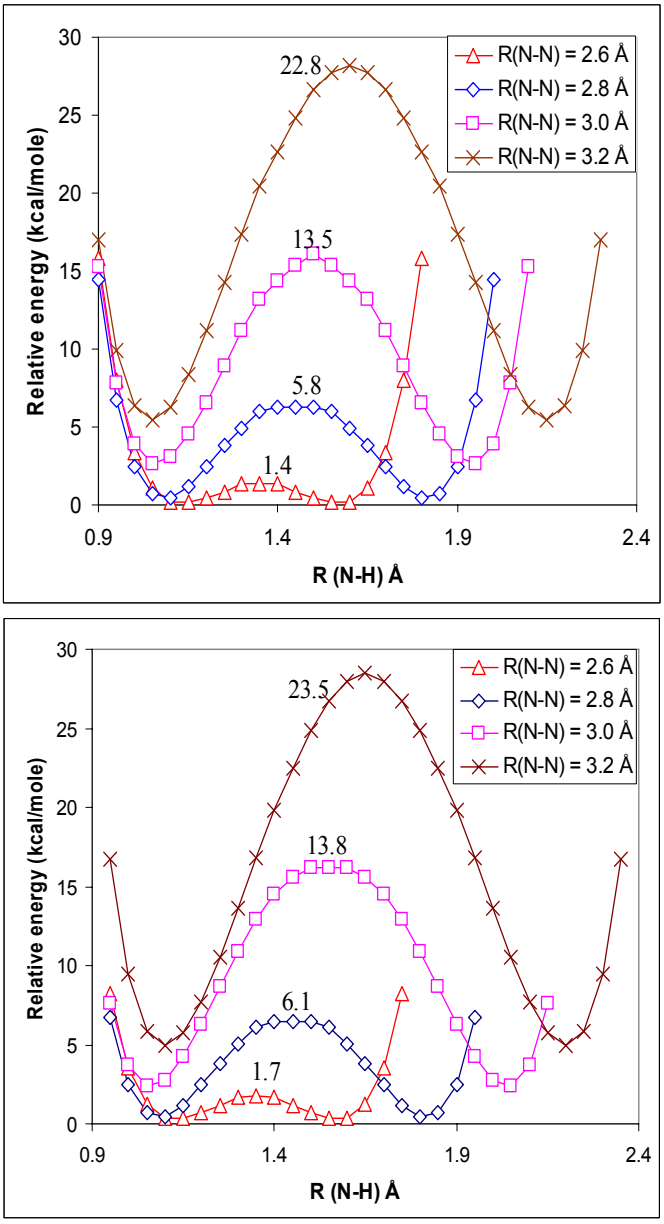


Figure S5. Energy for the proton transfer along the H reaction coordinate, for different donor N and acceptor N distances R(N-N). The results of this figure correspond to vacuum calculations.

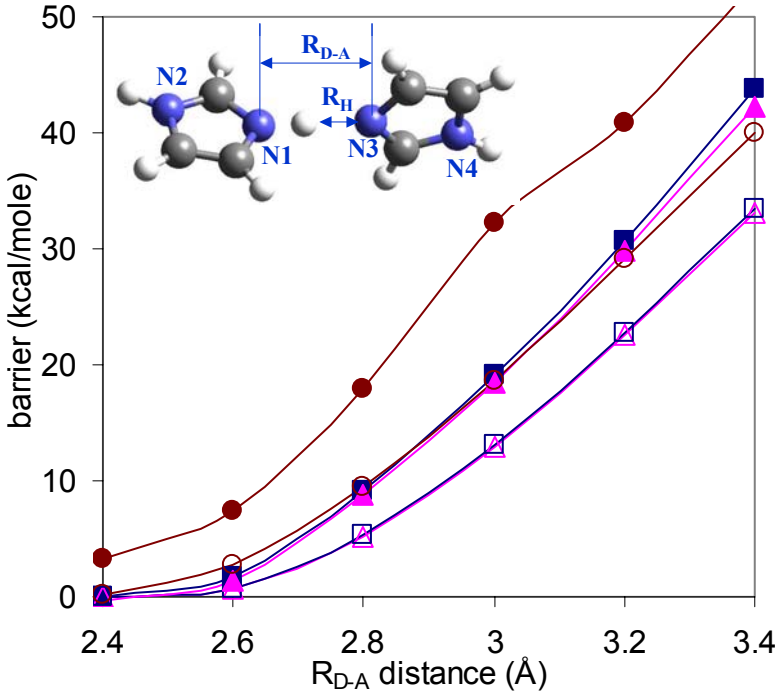


Figure S6. Proton hopping barriers with and without solvent correction. Red circles are proton hopping barriers between water dimers; Blue squares are proton hopping barriers between imidazole dimers; Magenta triangles are proton hopping barriers between trifluoroimidazoles dimers. Solid are data after solvent correction. Hollow are vacuum data without solvent correction.

In Figure S5, we show the curve without solvent correction. As in our calculation, we fitted barrier as an equation of distance between donor and acceptor.

For water; $E(r) = 26.57r^2 + 1.92r - 3.51$ kcal/mole

For imidazole; $E(r) = 38.40r^2 + 2.30r - 0.99$ kcal/mole

For tri-fluoro-imidazole; $E(r) = 37.27r^2 + 2.30r - 1.24$ kcal/mole

These equations were used to calculate energy barriers $E_{ij}(r)$ in equation (1) in text shown as below;

$$k_{ij}(r) = \kappa(T,r)\frac{k_B T}{h}\exp(-\frac{E_{ij}(r) - 1/2h\omega(r)}{RT})$$

Considering a particle hops distance *r* with hop rate *k* each time, the diffuse coefficient can be written as:

$$D = kr^2 \tag{2}$$

Therefore, for the case only considering proton hopping between carriers, the diffusion coefficient can be computed from the jump rates:

$$D_H = \frac{1}{6Nt}\int_0^{t\to\infty}\sum_i^N\sum_j^M k_{ij} r_{ij}^2 P_{ij} dt \tag{3}$$

where $k_{ij}$ is the hopping rate from the *i*th protonated carrier to the *j*th neutral one, and the summation is taken over all possible values of *i* and *j*. P*ij* is the probability of an ion being able to jump from site i to site j, and is defined by

$$P_{ij} = \frac{k_{ij}}{\sum_j^M k_{ij}}$$

We computed the distances between all pairs of donor and acceptors from the equilibrium molecular dynamics trajectory, and used Equation 3 to compute $D_H$. The distribution of distances between donor and acceptor N over the equilibrium trajectories for the Im/Nafion and ImF3/Nafion membranes is represented also in Figure 2b of the paper.

**2.3 Orientational correlation times for proton carriers in Nafion membranes.**

We computed the rotational correlation times from the integral of the first order orientational autocorrelation function $C_1$ for the vector formed by the two nitrogen atoms of each heterocycle:

$$C_1(t) = \frac{1}{N}\sum_{i=1}^{N}\langle \cos(\theta_i(t)) \rangle \quad (4)$$

where $N$ is the number of molecules of a given species (Im, $ImH^+$, ImF3, or $ImF3H^+$), $\theta(t)$ is the angle rotated by the unit intramolecular NN vector in a time interval $t$, and the brackets indicate an average over multiple origins along the 1 ns equilibrium trajectory. Figure S6 shows $C_1(t)$ for the protonated and neutral carriers in the Nafion membrane at 450 K.

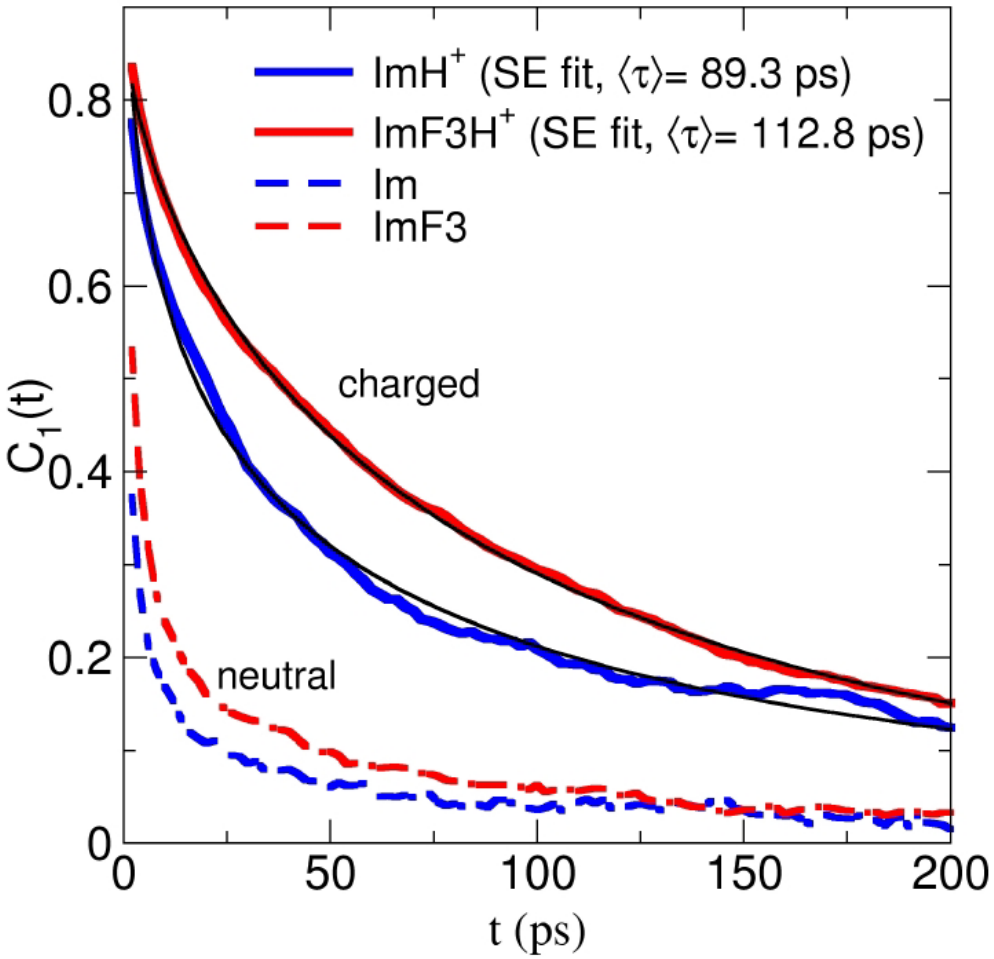

Figure S7. First order orientational correlation function for the unit vector that connects the two N atoms in the heter-cycle ring. Names as in the text. The black lines correspond to the best Stretched Exponential (SE) fits.

As the noise of the data increases with time t, due to the poorer statistics, we followed the usual custom of fitting the autocorrelation function to a stretched exponential function,

$$C_1(t) = Ae^{-(t/\tau)^{\beta}} \tag{5}$$

and computed the correlation time analytically from

$$\bar{\tau} = \frac{\tau}{\beta}\Gamma\left(\frac{1}{\beta}\right) \tag{6}$$

The resultant characteristic times for the rotation of the NN versor of the molecule are comparable for the hydrogenated and fluorinated species: 89.3 ps for imidazolium and 112.8 ps for trifluoroimidazolium.

References

(1). Accelrys_Inc Cerius2 Modeling Environment, Release 4.0; Accelrys Inc.: San Diego, 1999.

(2) Perdew, J. P.; Chevary, J. A.; Vosko, S. H.; Jackson, K. A.; Pederson, M. R.; Singh, D. J. and Fiohals, C. Phys. Rev. B 1992, 46, 6671.

(3) Lin, J. S.; Qteish, A.; Payne, M. C.; and Heine, V.; Phys. Rev. B 1993, 47, 4174.

(4) Plimpton, S. J. J. Comp. Phys. 1995, 117, 1.

(5) Plimpton, S. J.; Pollock, R.; Stevens, M. In the Eighth SIAM Conference on Parallel Processing for Scientific Computing: Minneapolis, 1997.

(6) Verlet, L. Phys. Rev. 1967, 159, 98.

(7) Hockney, Roger W.; Eastwood, James W. Computer simulation using particles; McGraw-Hill International Book Co.: New York, 1981.

(8) Mayo, S. L.; Olafson, B. D.; Goddard, William. A. J. Phys. Chem. 1990, 94, 8897.

(9) Jang, Seung Soon; Blanco, Mario; Goddard, William A.; Caldwell, Gregg; Ross, Richard B. Macromolecules 2003, 36, 5331.

(10) Levitt, Michael; Hirshberg, Miriam; Sharon, Ruth; Laidig, Keith E.; Daggett, Valerie J. Phys. Chem. B 1997, 101, 5051.

(11) Jang, Seung Soon; Molinero, Valeria; Cagin, Tahir; Goddard III, William A. J. Phys. Chem. B 2004, 108, 3149-3157.

(12) Geschke D, Bastug T, Jacob T, Fritzsche S, Sepp WD, Fricke B, Varga S, Anton J. , Phys. Rev. B 2001, 64, 235411

(13) Ogletree DF, van Hove MA, Somorjai GA, Surf. Sci, 1986, 173, 351.

(14) Blackman, G.S.; Ogletree, D.F.; van Hove, M.A.; and Somorjai, G. A.; Phys. Rev. Lett. 1988, 61, 2352.

(15) See http://www.vega-g.de/inh/e/en/DK-Wert-Liste_en.pdf